

## A 28 GHz 0.18- $\mu\text{m}$ CMOS cascade power amplifier with reverse body bias technique

A. F. Hasan<sup>\*1</sup>, S. A. Z. Murad<sup>2</sup>, F. A. Bakar<sup>3</sup>

<sup>1</sup>School of Microelectronic Engineering, Universiti Malaysia Perlis,  
Kampus Pauh Putra, Arau, Perlis, Malaysia

<sup>1,2,3</sup>Department of Electronic Engineering, Faculty of Engineering Technology, Universiti Malaysia Perlis,  
Kampus Unicity Alam, Sg. Chuchuh, Padang Besar, Malaysia

<sup>\*</sup>Corresponding author, e-mail: farizhasan@unimap.edu.my

### Abstract

A 28 GHz power amplifier (PA) using CMOS 0.18  $\mu\text{m}$  Silterra process technology is reported. The cascade configuration has been adopted to obtain high Power Added Efficiency (PAE). To achieve low power consumption, the input stage adopts reverse body bias technique. The simulation results show that the proposed PA consumes 32.03mW and power gain ( $S_{21}$ ) of 9.51 dB is achieved at 28 GHz. The PA achieves saturated power ( $P_{\text{sat}}$ ) of 11.10 dBm and maximum PAE of 16.55% with output 1-dB compression point ( $OP_{1\text{dB}}$ ) 8.44 dBm. These results demonstrate the proposed power amplifier architecture is suitable for 5G applications.

**Keywords:** 5G, CMOS power amplifier, low power consumption, power added efficiency, reverse body bias

Copyright © 2019 Universitas Ahmad Dahlan. All rights reserved.

### 1. Introduction

The race to deploy fifth generation (5G) wireless services by 2020 is ongoing and mm-wave technology will play a key role in meeting mounting demand for broadband data traffic [1]. The mm-wave become next generation carrier source due to exploding data growth in cellular networks and 26-60 GHz bands are of growing interest for potential 5G cellular network [2-4]. The global bandwidth shortage facing wireless carriers has motivated the exploration of the underutilized mm-wave frequency spectrum for future broadband cellular communication networks [5]. However, high efficiency silicon power amplifier (PA) for mm-wave communications is challenging due to ingrained trade-off between break-down and speed in silicon [6]. Power amplifier is one of the important element in Radio Frequency Integrated Circuit (RFIC) design to converts a low power radio frequency signal into a higher power signal in order to make sure that the RF system can deliver high quality, low latency video and multimedia applications for wireless devices [7, 8].

Many researches experience a lot of challenges in implementing mm-wave power amplifiers. First, it is harder to achieve high output power level due to the low supply voltage that accompanies smaller technology nodes. Besides, the technology shrinks causing the gate oxide become thinner and breakdown voltage become lower hence limit to get better output power at receiving end of the system [9, 10]. Second, the power gain output power tradeoff due to transistor sizing that presents itself at mm-wave frequencies poses an upper limit on the maximum transistor size that can be achieved with reasonably high gain and thus on the maximum output power of a single transistor [11]. Moreover, the power gain output power tradeoff due to impedance matching makes it more challenging to achieve high output power levels with reasonable power gain from a single stage amplifier [12, 13].

Research on fifth generation (5G) wireless services by 2020 is in progress, and mm-Wave Ka-Band technology will offer a vital role in meeting high demand for broadband data traffic [14, 15]. Recently, it is reported that Samsung's 5G network also adopts the 28 GHz mm-wave Ka-Band frequency. This is the triggering point for the researcher to research on Ka-Band mm-wave Power Amplifier (PA). These demands have promoted to comprehend a single chip radio transceiver in a low-cost CMOS technology with extra functionality [16]. Since the PA operates at very high frequency, it can have wide bandwidth. However, as the signal

bandwidth increases, the linearity of the PA is degraded because the asymmetric sideband is generated by the memory effect [6]. Furthermore, the critical part in designing CMOS PA in Ka-Band spectrum is to achieve high gain, low power, input and output matching and power added efficiency over wide band frequency from 26.5-40 GHz.

To date, several excellent CMOS PA's at 20-29 GHz have been reported [11-25]. For example a 22-29 GHz CMOS PA with 2 cascade cascode stage for high power gain in 0.18  $\mu\text{m}$  CMOS process technology is presented [14]. High saturated output power ( $P_{\text{sat}}$ ) of the PA can be enhanced by combining architecture adopted in the output stage. Though  $P_{\text{sat}}$  of 15.4 dBm is achieved, its PAE of 14.6% and DC power consumption of 163.8 mW are not good enough. In [15], a 22-27 CMOS PA with fully integrated transformer design in 0.18  $\mu\text{m}$  is reported. Though excellent power gain of 14 +/- 2 dB and  $P_{\text{sat}}$  of 17dBm is achieve, its PAE of 12% is not satisfactory. To demonstrate high PAE and low power consumption can be achieve simultaneously for a 28 GHz CMOS PA, in this work, we report a 28 GHz PA with excellent PAE,  $P_{\text{sat}}$  and low power consumption using 0.18  $\mu\text{m}$  Siltera process technology. The proposed PA comprises 3 cascade stages with reverse body bias design at input to achieve low dc power consumption and high PAE.

## 2. Circuit Design

The schematic design of cascade power amplifier is shown in Figure 1. Cascade topology has been chosen to provide sufficient gain. To achieve the desired output power at the power amplifier output, the transistor width of  $M_1$ ,  $M_2$  and  $M_3$  are optimize to be 48, 50 and 95  $\mu\text{m}$  respectively. The first stage consist of reverse body bias to control the power consumption at first stage ( $P_{\text{DC1}}$ ), to get the high efficiency and low power consumption. The output of the first stage PA is passed to the other stage through an inter-stage matching circuit formed by capacitors  $C_1$  and  $C_2$  which is designed and optimized to achieve maximum PAE and output power. Table 1 shows the component parameters for power amplifier schematic. The design with the three-stage of cascaded amplification is chosen to achieve the required gain. The output stage is designed to provide maximum output power while the first and second stages are designed for maximum gain. Figure 2 show block diagram of cascade system.

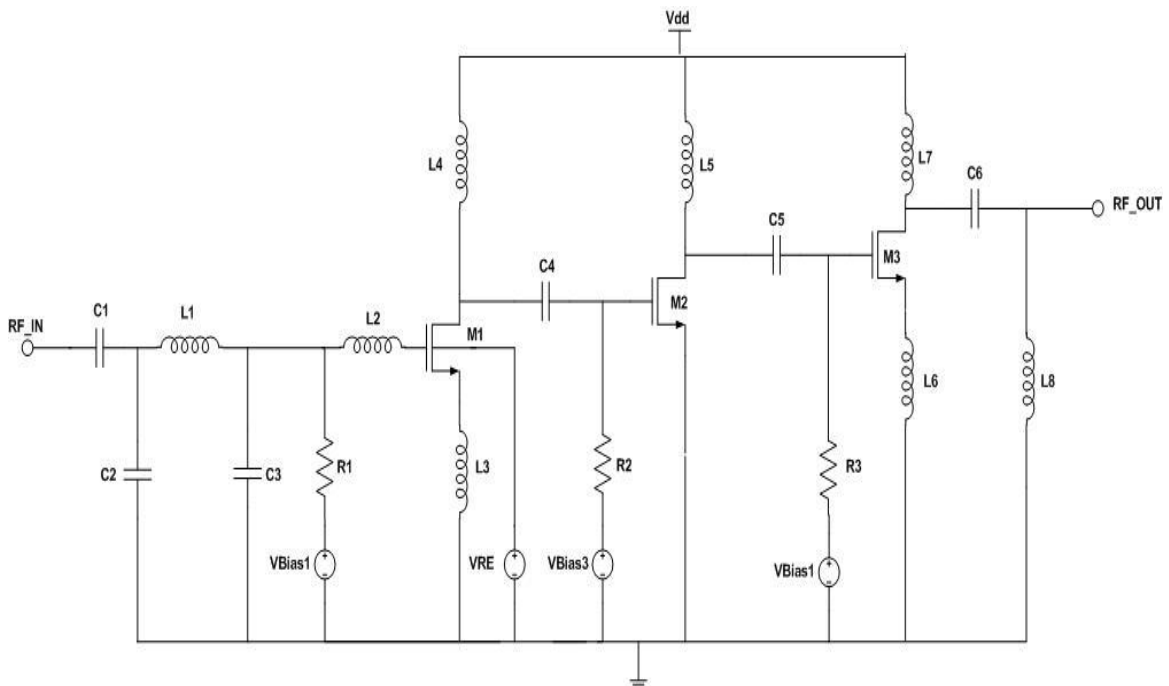


Figure 1. Complete schematic of the proposed three-stage CMOS PA

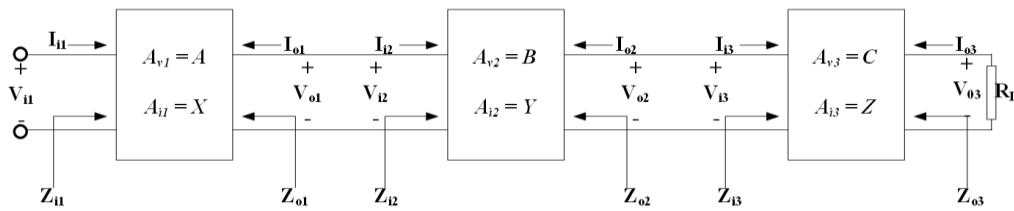


Figure 2. Block diagram of cascade system

Based on Figure 2:

$$\begin{aligned}
 A_v &= \frac{V_o}{V_i} = \frac{V_{o3}}{V_{i1}} \\
 &= \frac{V_{o3}}{V_{o2}} \times \frac{V_{o2}}{V_{o1}} \times \frac{V_{o1}}{V_{i1}} \\
 &= \frac{V_{o3}}{V_{i3}} \times \frac{V_{o2}}{V_{i2}} \times \frac{V_{o1}}{V_{i1}} \\
 &= A_{v1} A_{v2} A_{v3}
 \end{aligned} \tag{1}$$

therefore, if there is  $n^{\text{th}}$  stage:

$$A_v = \pm A_{v1} A_{v2} A_{v3} \dots A_{vn} \tag{2}$$

applying same concept to current gain:

$$A_i = \pm A_{i1} A_{i2} A_{i3} \dots A_{in} \tag{3}$$

knowing that, for power:

$$P = IV \tag{4}$$

Hence:

$$A_p = |A_i| |A_v| \tag{5}$$

as shown from (5), power gain of the cascade system increases due to current and voltage gain increased by cascading the amplifier stage. Therefore the need for cascading is important to maintain the power gain. The drain current,  $I_d$ , in the saturation region, depends on the W/L ratio of transistor, gate bias voltage ( $V_{gs}$ ) and threshold voltage ( $V_t$ ):

$$I_d = k' \frac{W}{L} \left[ (V_{gs} - V_t) V_{dsat} - \frac{V_{d,sat}^2}{2} \right] \tag{6}$$

where the threshold voltage defines as:

$$V_T = V_{TO} + \gamma (\sqrt{|-2\phi_F + V_{SB}|} - \sqrt{|-2\phi_F|}) \tag{7}$$

from (7), the source to bulk voltage ( $V_{SB}$ ) play an important role to control the  $V_T$ . As  $V_{SB}$  decreased,  $V_T$  will be increased resulting lower  $I_d$ . As  $I_d$  lower, total power consumption of the device ( $P_{DC}$ ) will be decreased, eventually it will drive to better efficiency of the circuit as power added efficiency (PAE) is depend on:

$$PAE = \frac{P_{out} - P_{in}}{P_{DC}} \quad (8)$$

noted that for cascade topology as shown in Figure 2, power gain of cascade can be written as:

$$G_1 = \frac{P_1}{P_{in}}, G_2 = \frac{P_{out}}{P_1} \quad (9)$$

from (9), the PAE of the first and second stage can be written as:

$$\eta_1 = \frac{P_1 - P_{in}}{P_{DC1}}, \eta_2 = \frac{P_{out} - P_1}{P_{DC2}} \quad (10)$$

hence;

$$\begin{aligned} \eta_{total} &= \frac{P_{out} - P_{in}}{P_{DC1} + P_{DC2}} \\ &= \frac{(P_{out} - P_1) + (P_1 - P_{in})}{P_{DC1} + P_{DC2}} \\ &= \frac{1}{P_{DC1} + P_{DC2}} [(P_{out} - P_1) + (P_1 - P_{in})] \end{aligned} \quad (11)$$

substituting (9) and (10) in (11) will lead to:

$$\eta_{total} = \frac{\eta_2}{\left[ \frac{P_{DC1}}{P_{DC2}} + 1 \right]} \left[ 1 + \left( \frac{G_1 - 1}{G_1} \right) \left( \frac{1}{G_2 - 1} \right) \right] \quad (12)$$

notice that, from (12) if the  $P_{DC1}$  is minimum and  $G_2$  is high, the efficiency of the PA will increased. Therefore, to reduce the  $P_{DC1}$ , reverse bias technique at the input stage is applied while  $G_2$  is set to be high by cascading the circuit.

Table 1. Component parameters for Power Amplifier schematic

| Component              | Parameter                             | Component       | Parameter       |
|------------------------|---------------------------------------|-----------------|-----------------|
| $V_{dd}$               | 1.9 V                                 | $C_5$           | 159.24 fF       |
| $V_{bias1}, V_{bias3}$ | 800 mV                                | $L_1$           | 478.98 pH       |
| $V_{bias2}$            | 864 mV                                | $L_2$           | 181.34 pH       |
| $V_{RE}$               | -510 mV                               | $L_3$           | 211.58 pH       |
| $M_1$                  | 0.18 $\mu\text{m}$ x 48 $\mu\text{m}$ | $L_4$           | 195.16 pH       |
| $M_2$                  | 0.18 $\mu\text{m}$ x 50 $\mu\text{m}$ | $L_5$           | 238.64 pH       |
| $M_3$                  | 0.18 $\mu\text{m}$ x 95 $\mu\text{m}$ | $L_6$           | 195.16 pH       |
| $C_1, C_2$             | 53.29 fF                              | $L_7$           | 208.93 pH       |
| $C_3$                  | 130 fF                                | $L_8$           | 705.34 pH       |
| $C_4$                  | 207.06 fF                             | $R_1, R_2, R_3$ | 2.15 k $\Omega$ |

### 3. Simulation Result and Discussion

S-parameter simulation results are shown in Figure 3. The power amplifier provides a simulated peak  $S_{21}$  of 9.51 dB at 26 GHz. The  $S_{21}$  3-dB bandwidth is 10 GHz centered around 26.75 GHz. As the input is matched to 50  $\Omega$  impedance, it provide a peak simulated  $S_{11}$  of -15 dB at 27 GHz. The  $S_{11}$  10-dB bandwidth is 3.48 GHz ranging from 25.52 GHz to 29 GHz.

As the output is matched to  $50\ \Omega$  impedance, it provides peak simulated  $S_{22}$  of  $-21.31\ \text{dB}$  at  $27.6\ \text{GHz}$ . The  $S_{22}$  10-dB bandwidth is  $12.43\ \text{GHz}$  ranging from  $25.41\ \text{GHz}$  to  $37.84\ \text{GHz}$ . Power simulation results are shown in Figure 4 and 5. The power amplifier delivers a 1 dB compression and saturated output powers of  $+8.44\ \text{dBm}$  and  $+11.10\ \text{dBm}$  respectively as shown in Figure 4. The power gain obtained for the designed PA is  $8.07\ \text{dB}$  and the peak simulated power added efficiency is  $16.55\%$  as shown in Figure 5. The amplifier consumes  $32.03\ \text{mW}$  from  $1.9\ \text{V}$  power supply.

Simulation results of the proposed PA, with and without reverse bias voltage at  $28\ \text{GHz}$  for PAE and DC power consumption is shown in Figure 6 (a) and (b). It is clearly notice that the performance of the PA with reverse bias voltage shows significant improvements in term of PAE and total power consumption. The performance comparison between the proposed PA with and without reverse bias are summarize in Table 2.

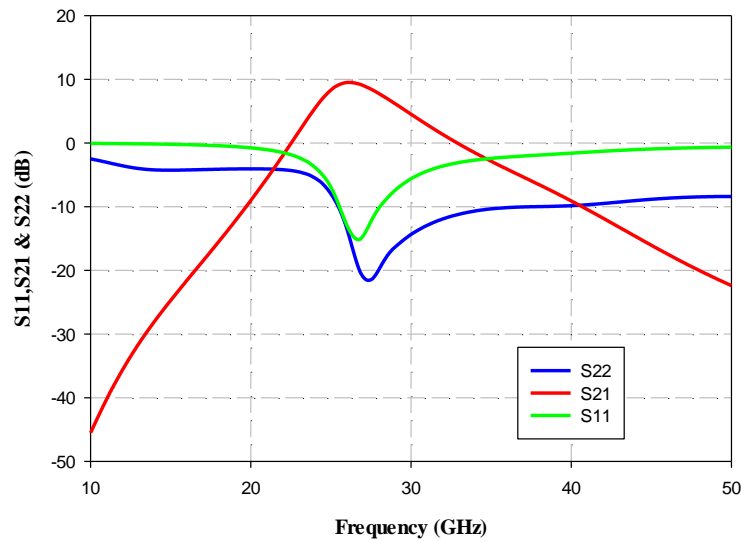


Figure 3. Simulated  $S_{21}$ ,  $S_{11}$  and  $S_{22}$  versus frequency at  $28\ \text{GHz}$

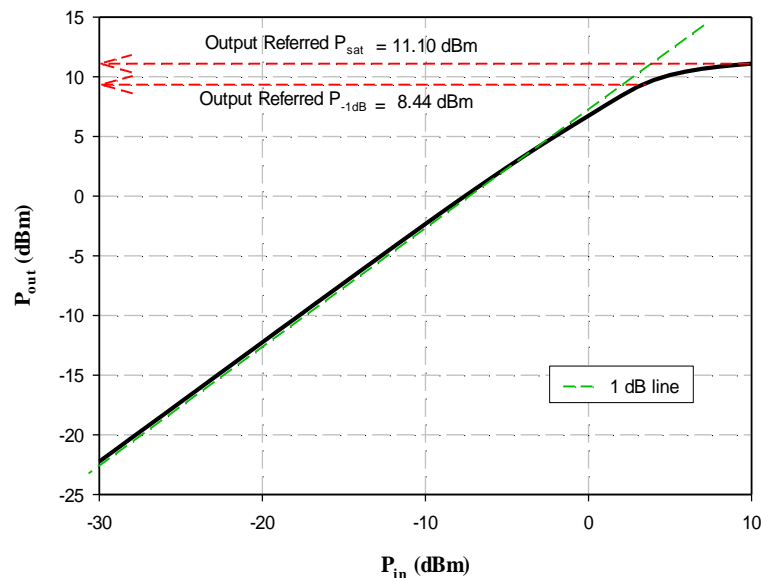


Figure 4. Simulated  $P_{1\text{dB}}$  of the PA at  $28\ \text{GHz}$

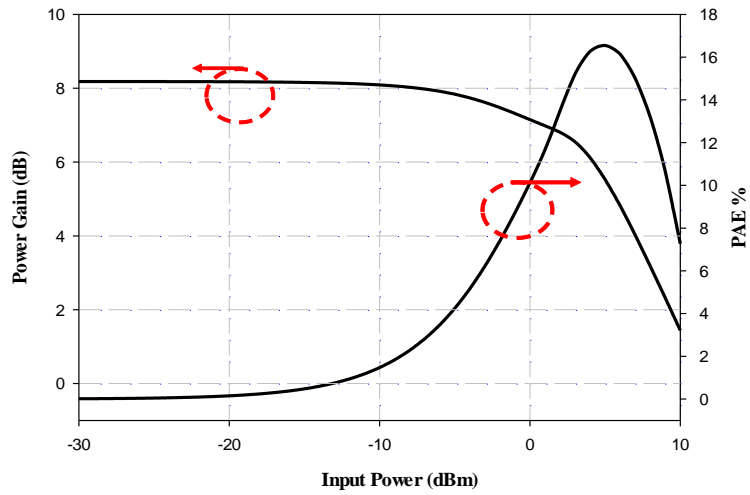
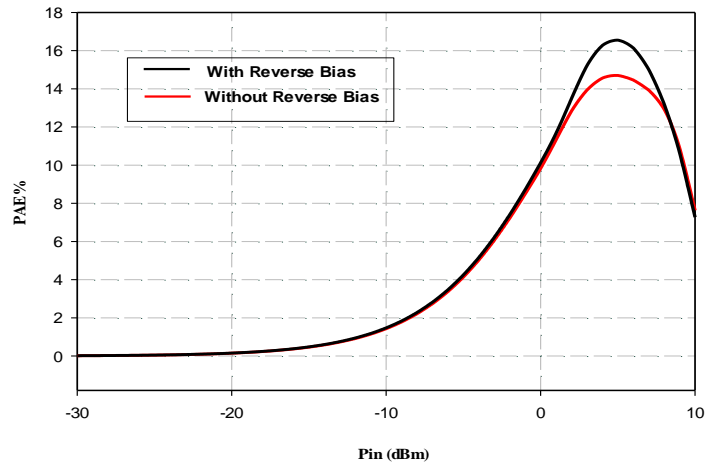
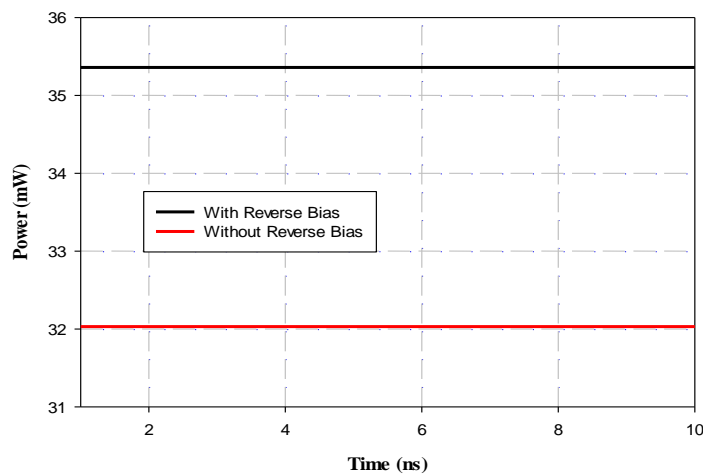


Figure 5. Simulated power gain & PAE of the PA at 28 GHz



(a)



(b)

Figure 6. Performance comparison between (a) PAE and (b) DC power, with and without reverse bias condition

Table 2. Summary of the Proposed PA's Performance at 28 GHz with and without Reverse Bias

| Variable                 | With Reverse Bias | Without Reverse Bias |
|--------------------------|-------------------|----------------------|
| Output P <sub>1</sub> dB | 8.44 dBm          | 8.72 dBm             |
| Output P <sub>sat</sub>  | 11.10 dBm         | 11.17 dBm            |
| Power Gain               | 8.07 dB           | 8.32 dB              |
| Maximum PAE              | 16.55 %           | 14.68%               |
| Peak S <sub>21</sub>     | 9.51 dB           | 9.30 dB              |
| Peak S <sub>11</sub>     | -15 dB            | -15 dB               |
| Peak S <sub>22</sub>     | -21.31 dB         | -20 dB               |
| DC power consumption     | 32.03 mW          | 35.36 mW             |

#### 4. Conclusion

This work addresses the requirements, and challenge of realizing an efficient mm-Wave PA in standard CMOS technology for 5G application. A 3 stage cascade with reverse bias topology at 28 GHz CMOS PA is presented. The amplifier is implemented in a standard CMOS 0.18  $\mu\text{m}$  process. The proposed topology employed cascade structure to obtain high PAE with reverse body bias at input stage to achieve low power consumption. The simulation results show that the proposed PA is able to deliver 11.10 dBm of output power to a 50  $\Omega$  load with PAE of 16.55% at power consumption of 32.03 mW using a 1.9 V voltage. The proposed PA can be used for future 5G communications.

#### Acknowledgements

The authors would like to express their highest gratitude to University Malaysia Perlis (UniMAP) and Malaysia Ministry of Higher Education (MOHE) for funding the PHD works.

#### References

- [1] S Onoe. *1.3 Evolution of 5G mobile technology toward 1 2020 and beyond*. in Digest of Technical Papers - IEEE International Solid-State Circuits Conference, 2016; 59: 23-28.
- [2] Hasan, AF, Murad, SAZ, Rani, KNA, Bakar, FA, Zulkifli, TZA. Study of CMOS power amplifier design techniques for ka-band applications. *Indonesian Journal of Electrical Engineering and Computer Science*. 2019; 13(2): 808-817.
- [3] S Shakib, HC Park, J Dunworth, V Aparin, K Entesari. *A 28GHz efficient linear power amplifier for 5G phased arrays in 28nm bulk CMOS*. in Digest of Technical Papers-IEEE International Solid-State Circuits Conference. 2016, vol. 59, pp. 352-353.
- [4] T Hanna, N Deltimple. *A Class-J Power Amplifier for 5G Applications in 28nm CMOS FD-SOI Technology*. in Proceedings of the 30th Symposium on Integrated Circuits and Systems Design. 2017: 1-4.
- [5] S Jin, M Kwon, K Moon, B Park, B Kim. Control of IMD asymmetry of CMOS power amplifier for broadband operation using wideband signal. *IEEE Trans. Microw. Theory Tech*. 2013; 61(10): 3753-3762.
- [6] M Franco, A Guida, A Katz, P Herczfeld. *Minimization of bias-induced memory effects in UHF radio frequency high power amplifiers with broadband signals*. in Proceedings-2007 IEEE Radio and Wireless Symposium. RWS, 2007: 369-372.
- [7] SAZ Murad, MF Ahamd, M Mohamad Shahimin, RC Ismail, KL Cheng, R Sapawi. *High Efficiency CMOS Class E Power Amplifier Using 0.13  $\mu\text{m}$  Technology*. Wireless Technology and Applications (ISWTA) 2012 IEEE Symposium on. 2012: 85-88.
- [8] SAZ Murad, RK Pokharel, H Kanaya, K Yoshida. *A 2.4 GHz 0.18- $\mu\text{m}$  CMOS Class E single-ended power amplifier without spiral inductors*. IEEE 2010 10th Topical Meeting on Silicon Monolithic Integrated Circuits in RF Systems (SIRF 2010). 2010: 25-28.
- [9] Sohiful Anuar Zainol Murad, Ramesh K Pokharel, Haruichi Kanaya, Keiji Yoshida and Oleg Nizhnik. *A 2.4-GHz 0.18- $\mu\text{m}$  CMOS Class E single-ended switching power amplifier with a self-biased cascode*. *Int. J. Electronic. Commun. (AEU)*. 2010; 64: 813-818.
- [10] A Chakrabarti, H Krishnaswamy. High-power high-efficiency class-E-like stacked mmWave PAs in SOI and Bulk CMOS: Theory and implementation. *IEEE Trans. Microw. Theory Tech*. 2014; 62(8): 1686-1704.
- [11] YN Jen, JH Tsai, CT Peng, TW Huang. *A 20 to 24 GHz +16.8 dBm Fully Integrated Power Amplifier Using 0.18  $\mu\text{m}$  CMOS Process*. *Microw. Wirel. Components Lett. IEEE*. 2009; 19(1): 42-44.
- [12] P Huang, Z Tsai, K Lin, H Wang, R Road. *A 22-dBm 24-GHz power amplifier using 0.18- $\mu\text{m}$  CMOS technology*. *2010 IEEE MTT-S International Microwave Symposium*. 2010; 1: 248-251.

- [13] KA Hsieh, HS Wu, KH Tsai, CK Clive Tzuang. A dual-band 10/24-GHz amplifier design incorporating dual-frequency complex load matching. *IEEE Trans. Microw. Theory Tech.*, 2012; 60(6 PART 1): 1649-1657.
- [14] T Huang, Y Lin, H Wang. A K-Band Adaptive-Bias Power Amplifier with Enhanced Linearizer Using 0.18 $\mu$ m CMOS Process. *IEEE MTT-S International Microwave Symposium 2015*. 2015; 4-6.
- [15] JL Kuo, H Wang. A 24 GHz CMOS power amplifier using reversed body bias technique to improve linearity and power added efficiency. *IEEE MTT-S Int. Microw. Symp. Dig.* 2012; 11-13.
- [16] SAZ Murad, RC Ismail, MNM Isa, M M Shahimin, M F Ahmad. High Efficiency CMOS Class-E Power Amplifiers in Gigahertz Frequencies: A Review. in *ARPN Journal of Engineering and Applied Sciences*. 2016; 11: 3866-3874.
- [17] Y-C Hsu, Y-S Chen, T-C Tsai, K-Y Lin. A K-band CMOS cascode power amplifier using optimal bias selection methodology. *Microw. Conf. Proc. (APMC)*. 2011: 793-796.
- [18] NC Kuo, JC Kao, CC Kuo, H Wang. K-band CMOS power amplifier with adaptive bias for enhancement in back-off efficiency. *IEEE MTT-S Int. Microw. Symp. Dig.* 2011: 3-6.
- [19] Y-S Lin, J-N Chang. A 24-GHz power amplifier with Psat of 15.9 dBm and PAE of 14.6% using standard 0.18  $\mu$ m CMOS technology. *Analog Integr. Circuits Signal Process.* 2014; 79(3): 427-435.
- [20] H Mosalam, A Allam, H Jia, A Abdelrahman, T Kaho, R Pokharel. A 12 to 24 GHz high efficiency fully integrated 0.18  $\mu$ m CMOS power amplifier. *IEICE Electronics Express*. 2016; 13(14): 1-10.
- [21] B Park, D Jeong, J Kim, Y Cho, K Moon, B Kim. Highly linear CMOS power amplifier for mm-wave applications. *IEEE MTT-S Int. Microw. Symp. Dig.* 2016: 16-18.
- [22] Y Huang, R Zhang, C Shi. A fully-integrated Ka-band CMOS power amplifier with Psat of 20 dBm and PAE of 19%. in 2016 IEEE International Conference on Ubiquitous Wireless Broadband, ICUWB 2016, 2016.
- [23] SY Mortazavi, KJ Koh. A 38 GHz inverse class-F power amplifier with 38.5% peak PAE, 16.5 dB gain, and 50 mW Psat in 0.13- $\mu$ m SiGe BiCMOS. *Dig. Pap. - IEEE Radio Freq. Integr. Circuits Symp.* 2015: 211-214.
- [24] JL Kuo, H Wang. A 24 GHz CMOS power amplifier using reversed body bias technique to improve linearity and power added efficiency. *IEEE MTT-S Int. Microw. Symp. Dig.* 2012: 11-13.
- [25] A Komijani, A Natarajan, A Hajimiri. A 24-GHz, +14.5-dBm fully integrated power amplifier in 0.18  $\mu$ m CMOS. *IEEE Journal of Solid-State Circuits*. 2005; 40(9): 1901-1908.